Journal of Materials Chemistry A

Accepted Manuscript

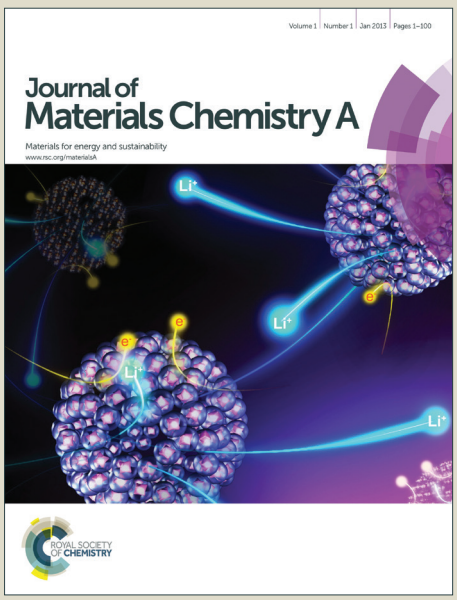

ROYAL SOCIETY OF CHEMISTRY

www.rsc.org/materialsA

Fullerene-Free Organic Photovoltaics Based on Unconvensional Material Combination: Molecular Donor and Polymeric Acceptor

Yanfang Geng[a], Bo Xiao[a], Seiichiro Izawa[b], Jianming Huang[b], Keisuke Tajima*[b], Qingdao Zeng[a], Erjun Zhou*[a]

[a] National Center for Nanoscience and Technology, Beijing 100190, P. R. China.

[b] Emergent Functional Polymers Research Team, RIKEN Center for Emergent Matter Science (CEMS), 2-1 Hirosawa, Wako 351-0198, Japan.

KEYWORDS. bulk heterojunction, non-fullerene, perylenediimide, polymeric materials, solar cells

ABSTRACT: In conventional organic photovoltaic cells, the active layer consists of a polymeric donor and a molecular acceptor (P_D/M_A). An unconventional material combination based on molecular donor/polymeric acceptor (M_D/P_A) emerged in 2014 but attracted limited attention. To broaden the photovoltaic material systems and understand the crucial factors related to the photovoltaic performance, in this report, we adopted a molecular donor (p-DTS(FBTTh$_2$)$_2$) and three polymeric acceptors based on perylenediimide (PDI). We find that the high contents (70-80%) of p-DTS(FBTTh$_2$)$_2$ and the better crystallinity and larger grains in the blend films induced by the addition of 1,8-diiodooctane (DIO) plays an important role in constructing the continuous and effective donor phase for the charge transfer and the hole transport in the active layers. The highest PCE of photovoltaic cells reached 3.01% with V_{OC} of 0.68 V, J_{SC} of 7.59 mA cm^{-2}, and FF of 0.58 for p-DTS(FBTTh$_2$)$_2$:PSe-PDI active layer, although the hole and the electron mobilities are still unbalanced. Further optimization of the film morphology and improvement of the electron mobility by material design and device engineering are expected to boost the efficiency of M_D/P_A type fullerene-free solar cells.

INTRODUCTION

Organic photovoltaic cells (OPVs) have received close attention from both academia and industry in recent years because of their unique advantages of low cost, light weight and capability to fabricate flexible large-area devices.[1-4] In the so-called bulk-heterojunction (BHJ) structure for OPVs, the active layers comprise a mixture of an electron donor (p-type) and an acceptor material (n-type). This structure provides both large interfaces for photo-generated excitons to efficiently dissociate into charge pairs and bicontinuous networks for transports of hole and electron to the corresponding electrodes.[2] From the viewpoint of the materials, fullerene derivatives are most frequently used as an effective electron acceptor, and power conversion efficiency (PCE) of over 10% has been achieved by using either polymer- or molecular-based donors.[5-11] However, recent developments of new n-type materials release us from the limitations of the fullerene-based acceptors such as the difficulty in the manipulations of the absorption spectra and the energy levels and the metastable morphology of the mixed films.[12] These limitations could be overcome by molecular designs of both polymer and molecular acceptor materials for non-fullerene BHJ.[13, 14]

In principle, there should not be any fundamental limitations of the material combinations in BHJ and there are four types categorized by the class of the materials: polymeric donor/molecular acceptor (P_D/M_A),[15-24] polymeric donor/polymeric acceptor (P_D/P_A, so-called "all-polymer"),[25-36] molecular donor/molecular acceptor(M_D/M_A, so-called "all-molecule") and molecular donor/polymeric acceptor (M_D/P_A). Due to the intense investigations and the large amount of promising polymer donors available, the first two types of OPV based on non-fullerene acceptors have achieved large success with the highest PCE of 6.80% and 6.71%, respectively.[22, 35] OPVs based on M_D/M_A could be traced back to 1986, where CuPc and PV molecules were used as the donor and the acceptor, respectively.[37] After that, owning to the developments of new molecular materials, the efficiency of OPVs based on M_D/M_A has been greatly improved.[38-41] In particular, the emergence of p-DTS(FBTTh$_2$)$_2$ in 2012 ignited the research on this type of OPVs. The OPVs based on p-DTS(FBTTh$_2$)$_2$ and a perylenediimide(PDI)-based molecular acceptor with PCE of 3.0% have been reported.[42-44] In recent report, the PCE of the M_D/M_A type OPV based on p-DTS(FBTTh$_2$)$_2$ shoot up to 5.4%.[45]

Compared with the above three types, OPVs based on M_D/P_A combinations are reported in very recent years and the number is still limited. In 2014, Zhan et al. reported the first M_D/P_A type OPV, using p-DTS(FBTTh$_2$)$_2$ as the donor and a PDI-based polymer as the acceptor, but PCE was as low as 0.29%.[46] Later, the same group changed the donor to DIB-SQ, a kind of squaraine dye, and simultaneously adopted a layer-by-layer fabrication method, and the efficiency of OPV was improved to 1.12%.[47] Almost at the same time, Nguyen et al. fabricated M_D/P_A type OPV based on p-DTS(FBTTh$_2$)$_2$ and a high performance naphthalenediimide (NDI)-based n-type polymer P(NDI2OD-T2) to achieve PCE of 2.1% by intensive device optimizations.[48] Recently, Inganäs et al. synthesized a

new donor small molecule DTD, and the PCE of the cells reached 3.6% by combining with P(NDI2OD-T2) as the acceptor.[49] More recently, Jo et al. obtained high PCE of 4.82% based on the combination of DTP-DPP with P(NDI2OD-T2).[50] So far, the highest PCE in reported OPVs based on M_D/P_A combinations, 1.12% for PDI-based polymer and 4.82% for NDI-based polymer, are inferior to those of other three types of OPVs. The vital factors that determine the miscibility, film morphology, charge transport and the device performance of M_D/P_A type devices are still not clear. There is still large room for investigations in M_D/P_A combinations to understand the mechanism of the formation of BHJ structures and to realize higher photovoltaic performance.

In this contribution, we utilized p-DTS(FBTTh$_2$)$_2$ as the molecular donor and three kinds of PX-PDI (X = C, T, Se) polymers based on PDI with different energy levels and band gaps as the acceptor to fabricate M_D/P_A type BHJ OPVs and systematically investigate the critical parameters related to the performance. The effect of solvent additives in the solution on the absorption spectra, the morphology of the blend films, charge transport properties and photovoltaic performance were also investigated.

RESULTS AND DISCUSSION

The chemical structures and energy levels of the materials used in this study are shown in Figure 1. Both the lowest unoccupied molecular orbitals (LUMO) and the highest occupies molecular orbitals (HOMO) energy levels were estimated by using cyclic voltammetry (CV) method according to the equations of LUMO = $-e(\varphi_{red} + 4.8)$ (eV) and HOMO = $-e(\varphi_{ox} + 4.8)$ (eV), where φ_{red} and φ_{ox} are the onset of reduction and oxidation potentials *vs*. Fc/Fc$^+$, respectively.[27] The LUMO energy of PC-PDI (−3.66 eV), PT-PDI (−3.94 eV) and PSe-PDI (−3.97 eV) are well below that of LUMO of p-DTS(FBTTh$_2$)$_2$ (−3.34 eV), thus effective electron transfer from the photoexcited donor to the acceptors can be expected. In addition, the HOMO energy offsets in of PC-PDI (0.71 eV), PT-PDI (0.72 eV) and PSe-PDI (0.63 eV) relative to HOMO of p-DTS(FBTTh$_2$)$_2$ are sufficiently high to promote the hole transfer from the polymeric acceptors to the molecular donor by photoexcitation of the acceptors. Therefore, we could expect the photocurrent generation from both the donor and the acceptor absorptions.

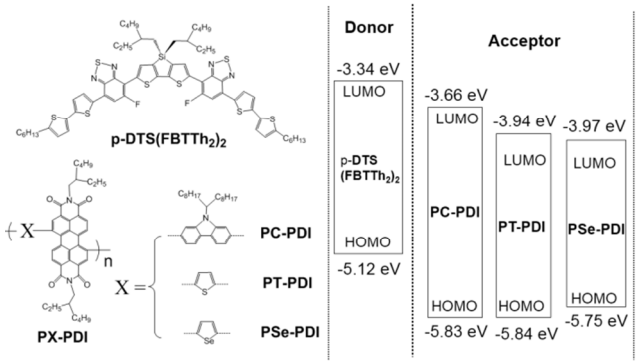

Figure 1. Chemical structures and orbital energy levels of p-DTS(FBTTh$_2$)$_2$ and three PDI-based polymers.

OPVs were fabricated with a conventional sandwich structure of glass/ITO/PEDOT:PSS/active layer/Ca/Al to investigate the photovoltaic performance of the three combinations. The device performances were optimized by varying the solvents, the molar ratios of the donor and the acceptors in the blends and the use of diiodooctane (DIO) as an additive in the solutions. The *J-V* curves under the light irradiation are shown in Figure 2 for the optimal devices and V_{OC}, J_{SC}, fill factor (FF), and PCE calculated from the *J-V* curves are summarized in Table 1 for the best conditions and in Table S1 for the various conditions. The PCE of the devices with the donor of PC-PDI, PT-PDI and PSe-PDI increase from 1.05%, 0.39% and 0.73%, respectively to 2.45%, 2.02% and 3.01%, respectively with addition of 0.5vol% of DIO in CB in the coating solutions. For these three combinations, the efficiencies are peaked with 0.5vol% of DIO, and the J_{SC} values largely decreased when the amount of DIO is more or less than this value. The best donor:acceptor ratio between p-DTS(FBTTh$_2$)$_2$ and PC-PDI, PT-PDI and PSe-PDI system were 7:3, 7:3 and 8:2, respectively, which are quite different from the other three fullerene-free OPV systems in which the typically optimal ratios are around 1:1. This high optimum contents of p-DTS(FBTTh$_2$)$_2$ in M_D/P_A system suggest large contents of the molecular materials might be necessary to construct both large interface area and continuous phase of the molecular materials phase which are suitable for OPVs.

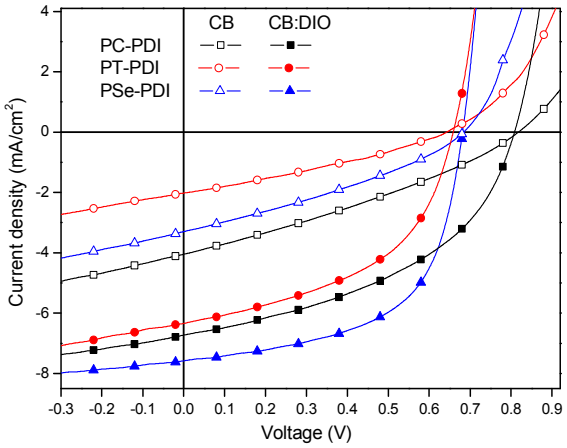

Figure 2. *J-V* curves under an AM 1.5 illumination (100 mW cm^{-2}) for OPVs based on p-DTS(FBTTh$_2$)$_2$:PX-PDI combinations spin-coated from CB or CB:DIO (0.5vol%) solutions.

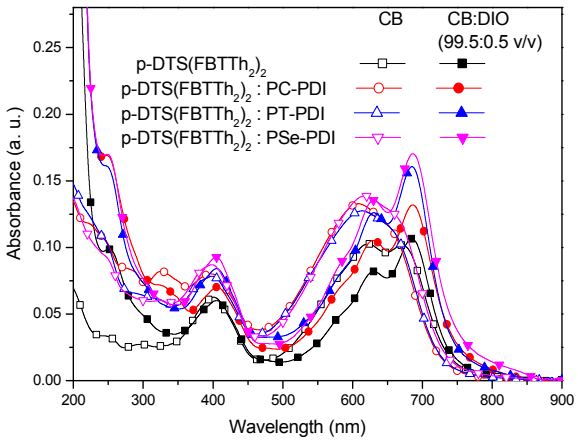

Figure 3. The absorption spectra of pristine p-DTS(FBTTh$_2$)$_2$ and blend films p-DTS(FBTTh$_2$)$_2$:PX-PDI combinations spin-coated from CB or CB:DIO solutions.

To investigate the effect of DIO on the properties of blend films, we measured the UV-vis absorption spectra of pure p-DTS(FBTTh$_2$)$_2$ film and the three kinds of blend film of p-DTS(FBTTh$_2$)$_2$:PX-PDI with the best ratios for the photovoltaic cells spin-coated from CB or CB:DIO (0.5vol%) solutions as

Table 1. Device characteristics of OPVs and the hole and electron mobilities in the corresponding single-carrier devices fabricated from the blend of p-DTS(FBTTh$_2$)$_2$ and the PX-PDI polymers. (The average values were calculated from 5 devices with standard deviation for the measurements.)

Active layer			V_{OC} (ave.) (V)	J_{SC} (ave.) (mA cm^{-2})	FF (ave.) (%)	PCE (ave.) (%)	Hole mobility ($cm^2 V^{-1} S^{-1}$)	Electron mobility ($cm^2 V^{-1} S^{-1}$)
n-type polymers	Solvent	D:A (wt/wt)						
PC-PDI	CB	7:3	0.82 (0.82±0.01)	4.05 (4.01±0.01)	0.31 (0.31±0.01)	1.03 (1.02±0.02)	3.1×10^{-5}	4.1×10^{-6}
	CB：DIO (99.5/0.5 v/v)	7:3	0.80 (0.80±0.00)	6.73 (6.65±0.04)	0.46 (0.45±0.01)	2.45 (2.41±0.04)	3.5×10^{-4}	5.3×10^{-6}
PT-PDI	CB	7:3	0.64 (0.63±0.01)	2.02 (1.96±0.07)	0.30 (0.30±0.02)	0.39 (0.37±0.02)	6.8×10^{-6}	3.1×10^{-6}
	CB：DIO (99.5/0.5 v/v)	7:3	0.66 (0.66±0.01)	6.34 (6.26±0.06)	0.48 (0.48±0.01)	2.02 (1.97±0.04)	2.0×10^{-4}	4.5×10^{-6}
PSe-PDI	CB	8:2	0.68 (0.68±0.01)	3.30 (3.30±0.01)	0.33 (0.32±0.02)	0.73 (0.70±0.02)	5.6×10^{-5}	7.7×10^{-6}
	CB：DIO (99.5/0.5 v/v)	8:2	0.68 (0.68±0.01)	7.59 (7.53±0.12)	0.58 (0.57±0.01)	3.01 (2.95±0.04)	6.1×10^{-4}	9.3×10^{-6}

shown in Figure 3. Without DIO, pure p-DTS(FBTTh$_2$)$_2$ film exhibit two peaks at 622 nm and 671 nm, while the three blend films only show one broad peak at around 620 nm and the peaks at 670 nm are absent, implying a relatively disordered structure of p-DTS(FBTTh$_2$)$_2$. With 0.5vol% DIO as the additive, the red-shift of the peaks to 690 nm was observed for both pure p-DTS(FBTTh$_2$)$_2$ film and p-DTS(FBTTh$_2$)$_2$:PX-PDI blend films. We speculate that these changes result from the increase of crystallinity in p-DTS(FBTTh$_2$)$_2$ for both the pure and the blend films during film formation process. The influence of DIO on the aggregation of p-DTS(FBTTh$_2$)$_2$ might enhance the intermolecular order, which could be favorable to the hole transport in the blend films.

To investigate the improvement of p-DTS(FBTTh$_2$)$_2$ crystallinity, the crystal structures of the pure p-DTS(FBTTh$_2$)$_2$ film and the blend p-DTS(FBTTh$_2$)$_2$:PX-PDI films were measured by 2D grazing-incidence X-ray diffraction (GIXRD) and the images are shown in Figure 4. When the films are spin-coated from CB solutions, the blend films show weaker signals compared with the pure donor film, suggesting that the amorphous acceptor polymers disperse into the donor phase and disturb the crystallization of p-DTS(FBTTh$_2$)$_2$. When the films were prepared from CB:DIO solvent, the intensity of the signals both in the pure and the blend films become stronger, which imply that the addition of DIO helps to improve the crystallinity of the donor phase. On the other hand, the orientational disorder in p-DTS(FBTTh$_2$)$_2$ become larger with DIO judging by the broadening of the diffraction peaks in the azimuth direction. Note that PX-PDIs do not show any diffraction peaks even in the pure films (data not shown). From the changes of the absorption spectra and 2D GIXRD, we can conclude that the addition of DIO could increase the p-DTS(FBTTh$_2$)$_2$ crystallinity, which should be favorable for the charge transport.

The charge transport properties of the p-DTS(FBTTh$_2$)$_2$:PX-PDI blend films spin-coated from CB or CB:DIO solutions were estimated by the space-charge limited current (SCLC)

technique. Both the estimated hole and electron mobilities are summarized in Table 1, and the typical *J–V* curves are shown in the supporting information (Figure S1). It is clear that the hole mobilities of these blends exhibit higher values than those of the electron mobilities. Upon addition of DIO in the solution, the hole mobilities increased by one to two orders of magnitude, which indicates that the addition of DIO plays an important role in constructing the continuous donor phase in the active layers. The electron mobilities for all the blend films were observed in the range of 3.1×10^{-6}-9.3×10^{-6} $cm^2V^{-1}s^{-1}$. The addition of DIO additive just slightly increased the electron mobility, which are still much lower than the hole mobility. The enhanced hole and electron mobilities in the blend films could contribute to more efficient charge extraction and thus the higher FF. However, it is important to balance electron mobility and hole mobility in organic solar cells for good photovoltaic performance.[31] Therefore, improvements of the electron transport would further increase the device performance.

The efficiency of exciton dissociation at the donor/acceptor interface is estimated by photoluminescence (PL) spectra. The PL spectra of p-DTS($FBTTh_2$)$_2$:PX-PDI blend films with excitation at 610 nm and shown in Figure S2. It can be seen that PL intensity was quenched by >95% in the blend films relative to the pure donor film without DIO additive. This suggests that efficient charge transfer between p-DTS($FBTTh_2$)$_2$ and PX-PDI polymers occurred. The efficient PL quenching of the blend film spin-coated without DIO indicates homogeneous mixed blend films, which are favorable to the exciton dissociation. On the other hand, the PL intensity of the pure donor film with DIO addition was much lower than that without DIO, suggesting that the lower emission quantum yield of the film due to the change of the packing order observed in UV-vis spectra. This change of the quantum yield makes the quantitative evaluation of the quenching efficiency difficult. However, PL intensities of the blend films with DIO addition largely increased compared to those without DIO even the PL quantum yield with the higher structural order is lower. This change implies that the charge transfer at the donor/acceptor interface is much less efficient in the blend films casted from CB:DIO solutions. This change may be attributed to the large aggregation domain of the donor or the acceptor, which leads to longer exciton diffusion length during the lifetime. Efficiency of PL quenching decreased but J_{SC} increased with the addition of DIO, which suggests that charge transport in the blend films without DIO is more severe problem. Therefore, morphology of the blend films needs to be employed to further monitor the complete yield of free charge carrier in p-DTS($FBTTh_2$)$_2$:PX-PDI systems because it is widely believed that there are inevitable relationships between the morphology of the blend active layers and the solar cell performances.[16, 31, 51-55]

Atomic force microscopy (AFM) was performed to understand the morphological features of the blend films p-DTS($FBTTh_2$)$_2$:PX-PDI spin-coated from the solutions without and with DIO additive. As shown in Figure 5, the three p-DTS($FBTTh_2$)$_2$:PX-PDI blend films gave relatively smooth surface with the root mean squares (RMS) roughness of 1.40, 1.37 and 0.317 nm, respectively. The most effective mixing of p-DTS($FBTTh_2$)$_2$:PSe-PDI might result from the larger torsion angle between selenophene and PDI moieties.[56] When the blend films were spin-coated from CB:DIO (0.5v%) solutions, phase-separated surface morphology with larger domain size formed, and the RMS roughness increased to 3.36, 1.49 and 1.69 nm, respectively. The relatively homogeneously mixed p-DTS($FBTTh_2$)$_2$:PX-PDI films without DIO should be more favorable for the exciton diffusion to the interface than the phase-separated blend films with DIO additive.[57] Based on the PX-PDI concentration in the blend films, we deduced the large aggregated domain are the p-DTS($FBTTh_2$)$_2$-rich region, which might result from the effect of additive DIO on the crystallization of p-DTS($FBTTh_2$)$_2$.[43] It is consistent with SCLC and PL analysis above, which demonstrate that the addition of DIO enhance the charge transport, but decrease the efficiency of the exciton dissociation.

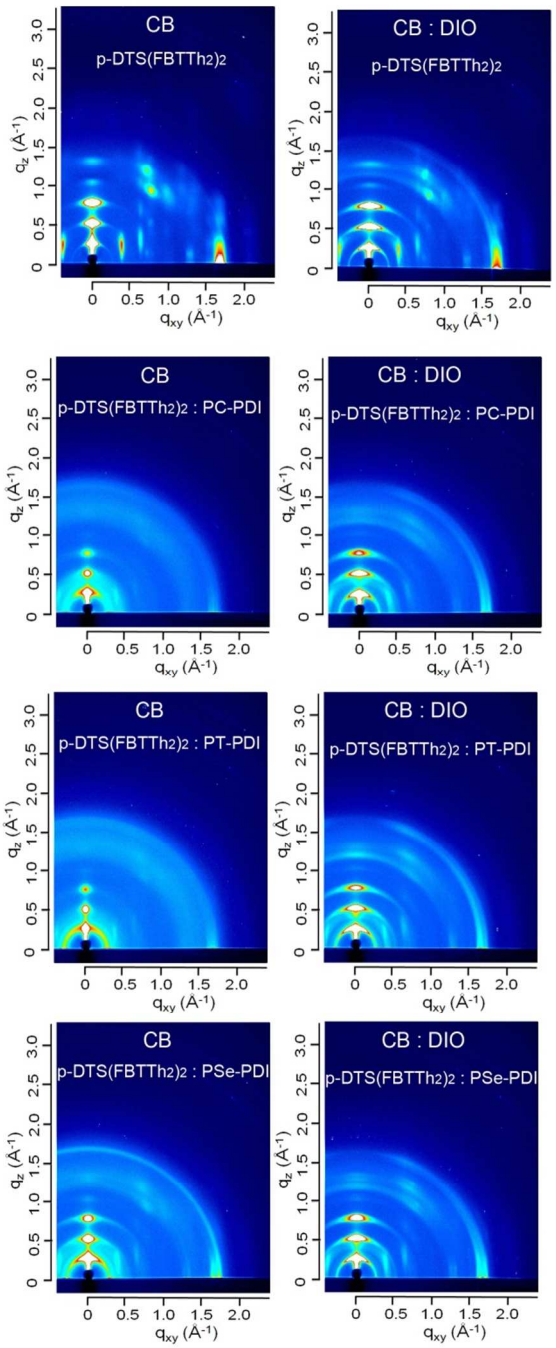

Figure 4. 2D GIXRD patterns of pure p-DTS($FBTTh_2$)$_2$ films and the blend films of p-DTS($FBTTh_2$)$_2$: PX-PDI spin-coated from CB or CB:DIO (0.5vol%) solutions.

External quantum efficiency (EQE) plots of the OPVs were shown in Figure 6. It is clear that these three photovoltaic devices showed a broad photocurrent response in 300~750 nm by using CB as solvent, but with low EQE value of <20%. The addition of DIO in the solutions drastically increases the EQE values, exhibiting a maximum value of about 40%. The absorption intensities of the films are quite similar between the films with and without DIO addition, so the difference in the EQE spectra could be due to the change in internal quantum efficiency (IQE). IQE can be considered as the product of the efficiencies for exciton diffusion to the donor/acceptor interface (η_{ED}), the charge transfer at the interface (η_{CT}), the charge dissociation into free charge carrier (η_{CD}) and the charge collection (η_{CC}).[57, 58] The addition of DIO could cause the decrease of η_{ED} through the larger domain size of the p-DTS(FBTTh$_2$)$_2$ suggested by AFM. Very recently, Nguyen et al. demonstrated that the length of exciton diffusion in p-DTS(FBTTh$_2$)$_2$ decrease from ~6.8 nm of the as-cast film to ~4.9 nm upon processing with DIO.[59] Both the effects could decrease η_{ED} with the addition of DIO. However, the enhanced hole mobility and crystallinity of p-DTS(FBTTh$_2$)$_2$ should largely increase the term of $\eta_{CT}\cdot\eta_{CD}\cdot\eta_{CC,}$ which could compensate the decreasing of η_{ED}. Thus, the EQE spectra in the region of 350-750 nm largely increased with the use of DIO for all the three material combinations.[60, 61]

CONCLUSIONS

In conclusion, we have fabricated fullerene-free OPVs based on unconventional materials combination, molecular donor and polymeric acceptors. The addition of DIO was effective to increase the crystallity of p-DTS(FBTTh$_2$)$_2$ and enhance the hole mobility of the blend films, which could compensate the inferior efficiency for exciton diffusion due to the change of the mixing morphology. The PCE of photovoltaic cells reached 3.01% with a V_{OC} of 0.68 V, a J_{SC} of 7.59 mA cm^{-2}, and a FF of 0.58 for p-DTS(FBTTh$_2$)$_2$:PSe-PDI active layer, where the ratio of p-DTS(FBTTh$_2$)$_2$ is as high as 80%. The use of M_D/P_A type combination opens up the new pathway to explore the materials for high performance OPVs.

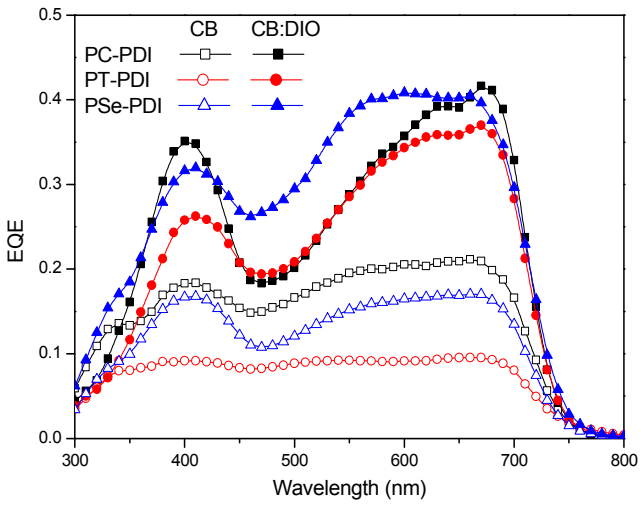

Figure 6. External quantum efficiency (EQE) plots of solar cells based on p-DTS(FBTTh$_2$)$_2$ and PX-PDI, spin-coated from CB or CB:DIO (0.5vol%) solutions.

EXPERIMENTAL SECTION

Materials. All chemicals were purchased from Alfa, Aldrich, TCI or Wako and used without further purification. The PDI-based copolymers PC-PDI, PT-PDI and PSe-PDI were synthesized according to the procedures in the literature.[27, 62]

Characterization. Absorption spectra were measured using a JASCO V-660 spectrometer. Atomic force microscopy (AFM) was conducted in tapping mode with a 5400 scanning

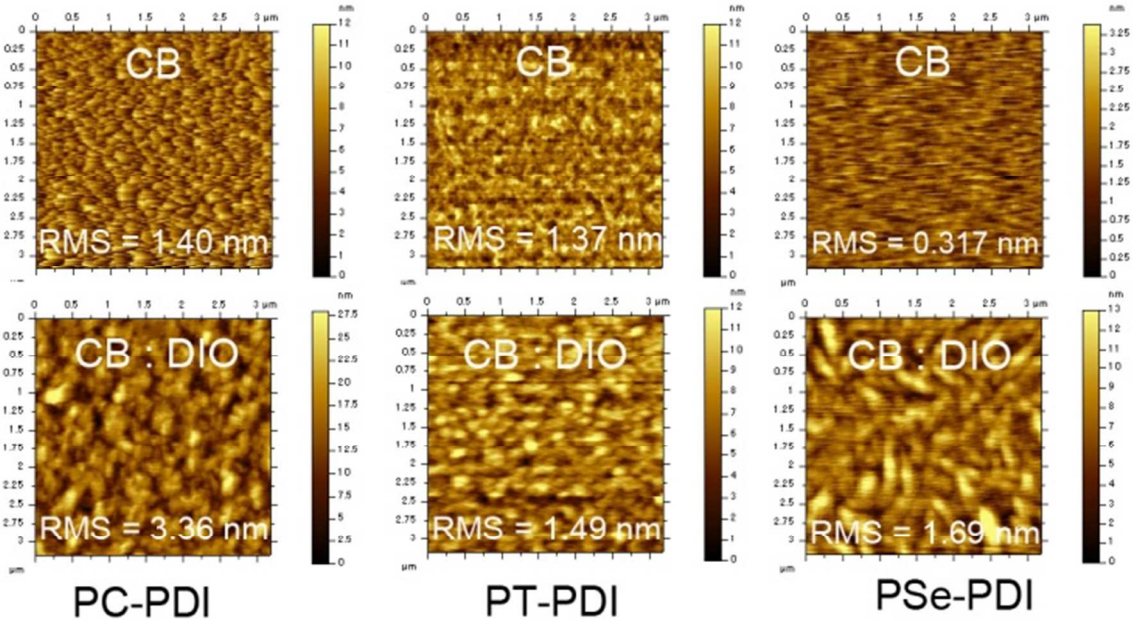

Figure 5. AFM topographical images with RMS roughness of M_D/P_A type solar cells based on p-DTS(FBTTh$_2$)$_2$:PX-PDI composite films spin-coated from different solvents, CB and CB:DIO (0.5vol%).

probe microscope (Agilent Technologies). 2D GIXRD patterns were measured at an incident angle of 0.12° using synchrotron radiation at beamline BL19B2 of SPring-8. The films were prepared by spin-coating chlorobenzene solutions (with or without DIO) of the polymers (10 g L^{-1}) on Si substrates and thermally annealed at 80 °C for 30 min.

Fabrication and characterization of M_D/P_A solar cells. Devices with the conventional sandwich structure were fabricated through the following steps. ITO-coated glass substrates were cleaned sequentially in detergent, water, acetone and 2-propanol by ultrasonication. PEDOT:PSS (Baytron P) was spin-coated (4000 rpm, 30 s) on ITO after drying the substrate. The film was dried at 150 °C under N_2 atmosphere for 5 min. After cooling the substrate, a blend solution of p-DTS(FBTTh$_2$)$_2$ and a PDI-based polymer with the total concentration of 20 g L^{-1} was spin-coated. The substrate was annealed at 80 °C for 30 min inside a nitrogen-filled glove box to dry the solvent completely, and then a Ca/Al (20 nm/60 nm) electrode was evaporated onto the substrate under high vacuum (10^{-4}-10^{-5} Pa) in an evaporation chamber (ALS Technology, H-2807 vacuum evaporation system with E-100 load lock). Photovoltaic cells without protective encapsulation were subsequently tested in air under simulated AM1.5 solar irradiation (100 mW cm^{-2}, Peccell Technologies, PCE-L11). The light intensity was adjusted by using a standard silicon solar cell with an optical filter (Bunkou Keiki, BS520). The current-voltage characteristics of the photovoltaic cells were measured using a Keithley 2400 I-V measurement system. The thickness of active layer was in the range of 100-120 nm measured by a Dektak 6M surface profilometer (ULVAC). The configuration of the shadow mask afforded eight independent devices on each substrate, with an active layer of ~0.21 cm^2 for each device. The effective area of the devices was defined using a metal photomask (2 mm × 3 mm) during irradiation with simulated solar light. The external quantum efficiency (EQE) of the devices was measured on a Hypermonolight System (Bunkou Keiki, SM-250F).

Hole and electron mobility measurement by space-charge-limited current (SCLC) method. Hole-and electron-only devices were fabricated by using the device structures of glass/ITO/PEDOT:PSS (30 nm) /active layer/MoO_3 (5 nm) /Au (60 nm) and glass/ Al (60 nm) /active layer /Al (60 nm), respectively. The active layers were spin-coated from chlorobenzene solution (with or without DIO) with the total concentration of 15 mg/mL. Both hole and electron mobility were calculated with the Mott−Gurney equation in the SCLC region (slope of 2 in the log$J$-log$V$ plots):

$$J = \frac{9}{8}\varepsilon_0\varepsilon_r\mu\frac{V^2}{L^3}$$

where ε_0 is the permittivity of the vacuum, ε_r is the dielectric constant of the polymer (assumed to be 3), L is the thickness of the polymer layer.

ASSOCIATED CONTENT

Supporting Information. device characteristics with different D/A molar ratio, J-V curves for the hole-only and electron-only devices. This material is available free of charge via the Internet at http://pubs.acs.org.

AUTHOR INFORMATION

Corresponding Author

* Corresponding author

E-mail: zhouej@nanoctr.cn; keisuke.tajima@riken.jp

ACKNOWLEDGMENT

2D GIXRD experiments were performed at beamline BL19B2 of SPring-8 with the approval of the Japan Synchrotron Radiation Research Institute (JASRI) (Proposal 2014B1583). The authors thank Dr. Tomoyuki Koganezawa (JASRI) for GIXRD measurements. This work was supported in part by the National Natural Science Foundation (No. 51473040, 51203030) and the New Energy and Industrial Technology Development Organization (NEDO), Japan.

REFERENCES

1. Y. Kim, S. Cook, S. M. Tuladhar, S. A. Choulis, J. Nelson, J. R. Durrant, D. D. C. Bradley, M. Giles, I. McCulloch, C. S. Ha and M. Ree, *Nat. Mater.*, 2006, 5, 197-203.
2. P. W. M. Blom, V. D. Mihailetchi, L. J. A. Koster and D. E. Markov, *Adv. Mater.*, 2007, 19, 1551-1566.
3. J. W. Chen and Y. Cao, *Acc. Chem. Res.*, 2009, 42, 1709-1718.
4. J. Roncali, *Acc. Chem. Res.*, 2009, 42, 1719-1730.
5. M. C. Scharber, D. Wuhlbacher, M. Koppe, P. Denk, C. Waldauf, A. J. Heeger and C. L. Brabec, *Adv. Mater.*, 2006, 18, 789-794.
6. C. J. Brabec, S. Gowrisanker, J. J. M. Halls, D. Laird, S. J. Jia and S. P. Williams, *Adv. Mater.*, 2010, 22, 3839-3856.
7. Y. Liu, J. Zhao, Z. Li, C. Mu, W. Ma, H. Hu, K. Jiang, H. Lin, H. Ade and H. Yan, *Nat. Commun.*, 2014, 5, 5293.
8. I. Etxebarria, J. Ajuria and R. Pacios, *Org. Electron.*, 2015, 19, 34-60.
9. Q. Zhang, B. Kan, F. Liu, G. Long, X. Wan, X. Chen, Y. Zuo, W. Ni, H. Zhang, M. Li, Z. Hu, F. Huang, Y. Cao, Z. Liang, M. Zhang, T. P. Russell and Y. Chen, *Nat. Photonics*, 2015, 9, 35-41.
10. Z. He, B. Xiao, F. Liu, H. Wu, Y. Yang, S. Xiao, C. Wang, T. P. Russell and Y. Cao, *Nat. Photonics*, 2015, 9, 174-179.
11. V. Vohra, K. Kawashima, T. Kakara, T. Koganezawa, I. Osaka, K. Takimiya and H. Murata, *Nat. Photonics*, 2015, 9, 403-408.
12. Y. Lin and X. Zhan, *Mat. Horiz.*, 2014, 1, 470-488.
13. X. Zhan, A. Facchetti, S. Barlow, T. J. Marks, M. A. Ratner, M. R. Wasielewski and S. R. Marder, *Adv. Mater.*, 2011, 23, 268-284.
14. X. Zhao and X. Zhan, *Chem. Soc. Rev.*, 2011, 40, 3728-3743.
15. P. Sonar, J. P. F. Lim and K. L. Chan, *Energy Environ. Sci.*, 2011, 4, 1558-1574.
16. G. Q. Ren, E. Ahmed and S. A. Jenekhe, *Adv. Energy Mater.*, 2011, 1, 946-953.
17. P. E. Schwenn, K. Gui, A. M. Nardes, K. B. Krueger, K. H. Lee, K. Mutkins, H. Rubinstein-Dunlop, P. E. Shaw, N. Kopidakis, P. L. Burn and P. Meredith, *Adv. Energy Mater.*, 2011, 1, 73-81.
18. T. Zhou, T. Jia, B. Kang, F. Li, M. Fahlman and Y. Wang, *Adv. Energy Mater.*, 2011, 1, 431-439.
19. Y. Zhou, L. Ding, K. Shi, Y. Z. Dai, N. Ai, J. Wang and J. Pei, *Adv. Mater.*, 2012, 24, 957-961.
20. X. Zhang, Z. H. Lu, L. Ye, C. L. Zhan, J. H. Hou, S. Q. Zhang, B. Jiang, Y. Zhao, J. H. Huang, S. L. Zhang, Y.

Liu, Q. Shi, Y. Q. Liu and J. N. Yao, *Adv. Mater.*, 2013, 25, 5791-5797.
21. J. Zhao, Y. Li, H. Lin, Y. Liu, K. Jiang, C. Mu, T. Ma, J. Y. Lin Lai, H. Hu, D. Yu and H. Yan, *Energy Environ. Sci.*, 2015, 8, 520-525.
22. Y. Lin, J. Wang, Z.-G. Zhang, H. Bai, Y. Li, D. Zhu and X. Zhan, *Adv. Mater.*, 2015, 27, 1170-1174.
23. Y. Lin, Z.-G. Zhang, H. Bai, J. Wang, Y. Yao, Y. Li, D. Zhu and X. Zhan, *Energy Environ. Sci.*, 2015, 8, 610-616.
24. O. K. Kwon, J.-H. Park, S. K. Park and S. Y. Park, *Adv. Energy Mater.*, 2015, 5, 1400929.
25. A. Facchetti, *Mater. Today*, 2013, 16, 123-132.
26. X. Zhan, Z. a. Tan, B. Domercq, Z. An, X. Zhang, S. Barlow, Y. Li, D. Zhu, B. Kippelen and S. R. Marder, *J. Am. Chem. Soc.*, 2007, 129, 7246-7247.
27. E. Zhou, J. Cong, Q. Wei, K. Tajima, C. Yang and K. Hashimoto, *Angew. Chem. Int. Ed.*, 2011, 50, 2799-2803.
28. E. Zhou, J. Cong, M. Zhao, L. Zhang, K. Hashimoto and K. Tajima, *Chem. Commun.*, 2012, 48, 5283-5285.
29. E. Zhou, J. Cong, K. Hashimoto and K. Tajima, *Adv. Mater.*, 2013, 25, 6991-6996.
30. E. Zhou, M. Nakano, S. Izawa, J. Cong, I. Osaka, K. Takimiya and K. Tajima, *ACS Macro. Lett.*, 2014, 3, 872-875.
31. T. Earmme, Y.-J. Hwang, S. Subramaniyan and S. A. Jenekhe, *Adv. Mater.*, 2014, 26, 6080-6085.
32. P. Cheng, L. Ye, X. Zhao, J. Hou, Y. Li and X. Zhan, *Energy Environ. Sci.*, 2014, 7, 1351-1356.
33. Y. Geng, J. Huang, K. Tajima, Q. Zeng and E. Zhou, *Polymer*, 2015, 63, 164-169.
34. H. Kang, M. A. Uddin, C. Lee, K. H. Kim, T. L. Nguyen, W. Lee, Y. Li, C. Wang, H. Y. Woo and B. J. Kim, *J. Am. Chem. Soc.*, 2015, 137, 2359-2365.
35. J. W. Jung, J. W. Jo, C. C. Chueh, F. Liu, W. H. Jo, T. P. Russell and A. K. Y. Jen, *Adv. Mater.*, 2015, 27, 3310-3317.
36. Y. J. Hwang, T. Earmme, B. A. E. Courtright, F. N. Eberle and S. A. Jenekhe, *J. Am. Chem. Soc.*, 2015, 137, 4424-4434.
37. C. W. Tang, *Appl. Phys. Lett.*, 1986, 48, 183-185.
38. B. Walker, X. Han, C. Kim, A. Sellinger and T.-Q. Nguyen, *ACS Appl. Mater. Inter.*, 2012, 4, 244-250.
39. J. D. Douglas, M. S. Chen, J. R. Niskala, O. P. Lee, A. T. Yiu, E. P. Young and J. M. J. Fréchet, *Adv. Mater.*, 2014, 26, 4313-4319.
40. J. Huang, X. Wang, X. Zhang, Z. Niu, Z. Lu, B. Jiang, Y. Sun, C. Zhan and J. Yao, *ACS Appl. Mater. Inter.*, 2014, 6, 3853-3862.
41. Y. Lin, J. Wang, S. Dai, Y. Li, D. Zhu and X. Zhan, *Adv. Energy Mater.*, 2014, 4, 1400420.
42. A. Sharenko, C. M. Proctor, T. S. van der Poll, Z. B. Henson, T.-Q. Nguyen and G. C. Bazan, *Adv. Mater.*, 2013, 25, 4403-4406.
43. A. Sharenko, D. Gehrig, F. Laquai and T.-Q. Nguyen, *Chem. Mater.*, 2014, 26, 4109-4118.
44. Y. J. Kim, D. S. Chung and C. E. Park, *Nano Energy*, 2015, 15, 343-352.
45. O. K. Kwon, J.-H. Park, D. W. Kim, S. K. Park and S. Y. Park, *Adv. Mater.*, 2015, 27, 1951-1956.
46. P. Cheng, X. Zhao, W. Zhou, J. Hou, Y. Li and X. Zhan, *Org. Electron.*, 2014, 15, 2270-2276.
47. Y. Wang, X. Zhao and X. Zhan, *J. Mater. Chem. C*, 2015, 3, 447-452.
48. Z. Li, J. D. A. Lin, H. Phan, A. Sharenko, C. M. Proctor, P. Zalar, Z. Chen, A. Facchetti and T.-Q. Nguyen, *Adv. Func. Mater.*, 2014, 24, 6989-6998.
49. Z. Tang, B. Liu, A. Melianas, J. Bergqvist, W. Tress, Q. Y. Bao, D. P. Qian, O. Inganas and F. L. Zhang, *Adv. Mater.*, 2015, 27, 1900-1907.
50. J. W. Jung, T. P. Russell and W. H. Jo, *Chem. Mater.*, 2015, 27, 4865-4870.
51. S. Rajaram, P. B. Armstrong, B. J. Kim and J. M. J. Fréchet, *Chem. Mater.*, 2009, 21, 1775-1777.
52. M. Schubert, D. Dolfen, J. Frisch, S. Roland, R. Steyrleuthner, B. Stiller, Z. Chen, U. Scherf, N. Koch, A. Facchetti and D. Neher, *Adv. Energy Mater.*, 2012, 2, 369-380.
53. H. Yan, B. A. Collins, E. Gann, C. Wang, H. Ade and C. R. McNeill, *ACS Nano*, 2012, 6, 677-688.
54. K. D. Deshmukh, T. Qin, J. K. Gallaher, A. C. Y. Liu, E. Gann, K. O'Donnell, L. Thomsen, J. M. Hodgkiss, S. E. Watkins and C. R. McNeill, *Energy Environ. Sci.*, 2015, 8, 332-342.
55. C. Lee, H. Kang, W. Lee, T. Kim, K. H. Kim, H. Y. Woo, C. Wang and B. J. Kim, *Adv. Mater.*, 2015, 27, 2466-2471.
56. T. Earmme, Y. J. Hwang, N. M. Murari, S. Subramaniyan and S. A. Jenekhe, *J. Am. Chem. Soc.*, 2013, 135, 14960-14963.
57. J. Guo, H. Ohkita, H. Benten and S. Ito, *J. Am. Chem. Soc.*, 2010, 132, 6154-6164.
58. Y. Tamai, K. Tsuda, H. Ohkita, H. Benten and S. Ito, *Phys. Chem. Chem. Phys.*, 2014, 16, 20338-20346.
59. J. D. A. Lin, O. V. Mikhnenko, T. S. van der Poll, G. C. Bazan and N. Thuc-Quyen, *Adv. Mater.*, 2015, 27, 2528-2532.
60. T. S. van der Poll, J. A. Love, T. Q. Nguyen and G. C. Bazan, *Adv. Mater.*, 2012, 24, 3646-3649.
61. C. M. Proctor, M. Kuik and T.-Q. Nguyen, *Prog. Polym. Sci.*, 2013, 38, 1941-1960.
62. X. Wang, J. Huang, K. Tajima, B. Xiao and E. Zhou, *Mater. Today Commun.*, 2015, 4, 16-21.

TOC

Photovoltaic cells based on molecular donor/polymeric acceptors were investigated and 3.01% PCE was achieved by using DIO as additive.